

# An unsymmetric ligand framework for non-coupled homo- and heterobimetallic complexes.

Ruth M. Haas<sup>†</sup>, Zachary Hern<sup>‡</sup>, Stephen Sproules<sup>§</sup>, Corinna R. Hess<sup>†\*</sup>

<sup>†</sup>Technische Universität München, Department of Chemistry and Catalysis Research Center, Lichtenbergstraße 4, 85748 Garching, Germany

<sup>‡</sup>University of Texas at San Antonio, Department of Chemistry, San Antonio, Texas 78249, United States.

<sup>§</sup> University of Glasgow, School of Chemistry, University Avenue, Glasgow, G12 8QQ, U. K.

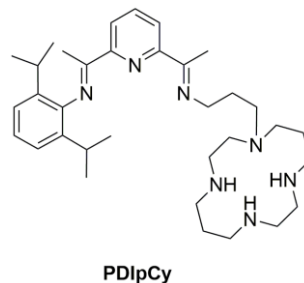
Supporting Information Placeholder

**ABSTRACT:** We herein introduce a new unsymmetric ligand, PDIpCy, that offers two distinct, non-coupled coordination sites. A series of homo- and hetero-bimetallic complexes,  $[\text{Zn}_2(\text{PDIpCy})(\text{THF})(\text{OTf})_4]$  (**1**),  $[\text{Ni}_2(\text{PDIpCy})(\text{THF})(\text{OTf})_2](\text{OTf})_2$  (**2**), and  $[\text{NiZn}(\text{PDIpCy})(\text{THF})(\text{OTf})_4]$  (**3**), are described. The compounds were structurally characterised and their redox properties were examined. The PDI unit of the ligand supports a number of ligand-centered redox processes. The one-electron reduced bimetallic compounds,  $[\text{Zn}_2(\text{PDIpCy})(\text{OTf})_3]$  (**4**),  $[\text{Ni}_2(\text{PDIpCy})(\text{OTf})](\text{OTf})_2$  (**5**), and  $[\text{NiZn}(\text{PDIpCy})(\text{OTf})_3]$  (**6**), were successfully isolated, and their electronic structures verified by absorption and EPR spectroscopy. The reduced compounds are charge-separated species, with electron storage at either the PDI ligand (**4**) or at the PDI-bound metal ion (**5**, **6**).

An impressive assortment of multi-nuclear complexes has been reported over the years, the synthesis of which frequently was motivated by multi-electron reaction targets (e.g.  $\text{O}_2$ ,  $\text{N}_2$  activation). Multi-metallic compounds may be ideally suited for chemistry involving manifold redox processes, as such systems offer a wider range of redox states and a more varied coordination environment than a single metal ion. Cooperative interactions between the metal centers also can be beneficial for reactivity. Indeed, the enzymes that catalyze small molecule reactions commonly employ multiple metal cofactors, and both of the aforementioned effects are key to the reactivity of the biological active sites.<sup>1</sup> Consequently, numerous biomimetic homo- and hetero-nuclear complexes have been synthesized in particular.<sup>1b, 2</sup>

A number of contemporary molecular design strategies have focused specifically on the assembly of varying combinations of metal ions that each adopt distinct coordination environments and functions. Notable examples include the growing series of M-M bonded complexes, which feature modular combinations of early to late transition metal ions and main group elements, encapsulated within a single ligand scaffold.<sup>3</sup> A number of unique unsymmetric ligands also have been synthesized, that support a neighbouring arrangement of two different transition metal ions via coupled M-Y-M motifs.<sup>4</sup> Multinuclear complexes that pair transition metal centers with alkali metal, alkaline earth elements or lanthanide binding sites – again, mainly via M-Y-M bridging motifs – also have become more abundant.<sup>5</sup> Such platforms with distinct metal binding sites offer advantages for reactivity.<sup>5b, 5d, 6</sup>

As part of our own efforts to generate complexes for multi-electron reactions, we now have synthesized a new ligand scaffold, PDIpCy (Scheme 1), that provides a platform for unsymmetric bimetallic compounds. The molecule contains two discrete coordination sites furnished by pyridyldiimine (PDI) and tetraaza-decane (cyclam; Cy) groups, separated by a flexible propyl linker. A related PDI-based ligand tethered to a crown ether unit for coordination of alkali metals was previously reported by Delgado et al.<sup>5c</sup> PDIpCy, however, was generated with the aim of binding transition metal ions at both coordination sites, and the potential to support redox reactivity at both centers; coordination complexes of each ligand type are well known.<sup>7</sup> and have demonstrated promise for reactions that include  $\text{CO}_2$  reduction,  $\text{H}_2$  evolution and olefin epoxidation.<sup>8</sup> PDIpCy offers a framework for *non-coupled* binuclear centers, in contrast to the aforementioned M-M and M-Y-M motifs. We envisioned that the motif would allow each metal center to individually be tuned both with respect to electronic properties and function. An additional feature of the PDIpCy ligand is the redox-active PDI group. The non-innocent unit can supply up to four electrons, independent of the coordinated metal. The combination of redox-active and -innocent ligands may permit charge-localization, enabling the formation of formal mixed valent compounds via ligand-centered reduction. We herein describe the first homo- and hetero-bimetallic Zn- and Ni-PDIpCy complexes, which provide initial insight into the coordination chemistry and redox properties of our new multidentate ligand.



**Scheme 1.** The unsymmetric ligand PDIpCy

PDIpCy was synthesized *via* two consecutive condensation reactions of 2,6-diacetylpyridine with 2,6-diisopropylaniline<sup>9</sup> and 3-(1,4,8,11-tetraazacyclotetradecan-1-yl)propan-1-amine, respectively (Scheme S1). The latter  $\text{N}_4$ -macrocyclic precursor was obtained by a Michael addition of acrylonitrile to cyclam, followed by reduction of the nitrile group using Raney nickel. Only 70% conversion to product was achieved in the final reaction step,

however, the target ligand was cleanly isolated upon recrystallization from acetonitrile at low temperatures ( $-30^{\circ}\text{C}$ ). The  $^1\text{H}$  NMR spectrum of PDIPCy (Figure S11) was assigned using additional data from  $^{13}\text{C}$ , COSY, HSQC and HMBC NMR measurements (Figures S12 – S15). Nearly all of the individual proton signals could be assigned, with the exception of the methylene protons of the cyclam group, most of which are encompassed by a broad multiplet at 2.50 – 2.78 ppm.

The bimetallic complexes were subsequently synthesized upon addition of  $\text{M}(\text{OTf})_2$  salts to PDIPCy (Scheme S2). The synthesis of the dizinc compound,  $[\text{Zn}_2(\text{PDIPCy})(\text{THF})(\text{OTf})_4]$  (**1**), proceeded at room temperature, whereas the coordination of nickel to generate  $[\text{Ni}_2(\text{PDIPCy})(\text{THF})(\text{OTf})_2](\text{OTf})_2$  (**2**) required heating of the reaction mixture ( $80^{\circ}\text{C}$ ). The heterobimetallic complex  $[\text{NiZn}(\text{PDIPCy})(\text{THF})(\text{OTf})_4]$  (**3**) was obtained by simultaneous addition of one equiv. of each  $\text{M}(\text{OTf})_2$  salt to the ligand in EtOH. The formation of the heterobimetallic complex was confirmed by mass spectrometry (MS, Figure S29 and S30). We also examined mixtures of **1** and **2**, to see whether exchange of the metal ions, and formation of **3**, can occur under various conditions (Figures S31 and S32). Metal ion exchange was not observed for mixtures of the homobimetallic complexes in MeCN at room temperature, as verified by MS. However, formation of the heterobimetallic species does occur upon heating of an MeCN solution ( $60^{\circ}\text{C}$ ), as well as in MeOH (rt and  $60^{\circ}\text{C}$ ).

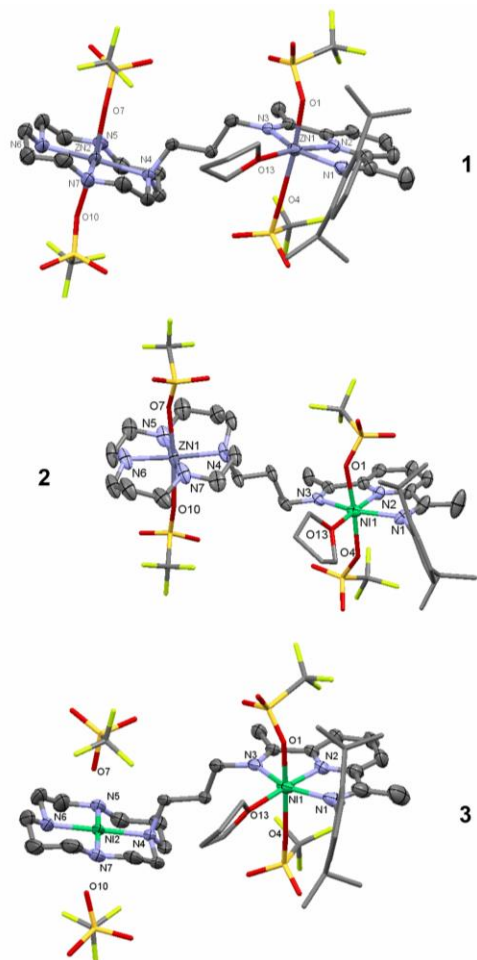


**Figure 1.** Molecular structures of **1** – **3** (50% probability ellipsoids). Hydrogen and solvent molecules are omitted for clarity.

Figure 1 depicts the molecular structures of all three binuclear compounds (see Table S1 – S2 for crystallographic information). The metal centers of **1** – **3** are separated by ca. 8 Å. Both Zn ions

of **1** adopt a six-coordinate tetragonal geometry. The N-atoms of the cyclam and PDI units form the equatorial plane of each site, with an additional THF molecule coordinated to  $\text{Zn}_{\text{PDI}}$ . Two triflate anions also are coordinated to each metal ion ( $\text{Zn}_{\text{PDI}}\cdots\text{O}_{\text{avg}} \sim 2.16$  Å;  $\text{Zn}_{\text{Cyclam}}\cdots\text{O}_{\text{avg}} \sim 2.32$  Å) in a *trans*-arrangement. The dinickel compound is structurally similar to **1**. However, the triflate ions localized near the cyclam unit are only weakly associated with the  $\text{Ni}^{\text{II}}$  ion ( $\text{Ni}_{\text{Cyclam}}\cdots\text{O}_{\text{avg}} \sim 2.7$  Å), such that the geometry of  $\text{Ni}_{\text{Cyclam}}$  is effectively square planar. The bond lengths of all Ni–N bonds of **2** are shorter than the analogous Zn–N distances, as expected given the smaller ionic radius of the  $\text{Zn}^{\text{II}}$  ion. The bond distances are in agreement with literature values for related mononuclear PDI and cyclam compounds.<sup>10</sup> The molecular structure of **3** highlights preferred coordination of the  $\text{Ni}^{\text{II}}$  ion to the PDI site, whereas the  $\text{N}_4$ -macrocycle is occupied by the zinc atom. As in **1** and **2**, the chiral cyclam adopts the R,S,S,R configuration. The macrocyclic unit is situated ‘above’ the plane of the M–PDI moiety, in contrast to its orientation in the homobimetallic structures.

The solution  $^1\text{H}$  NMR spectrum of the diamagnetic **1** (Figure S16) shows a slight upfield shift of all proton resonances, vs. the corresponding signals of the PDIPCy spectrum, due to the presence of the dicationic metal centers. Two distinct signals are observed for  $\text{H}_9$  and  $\text{H}_{18}$ , and several other resonances exhibit more complex splitting patterns, indicating an overall loss of symmetry upon coordination of the zinc ions. A signal for the coordinated THF molecule, as seen in the solid state structure, is not observed in the NMR spectrum. The solvent molecule appears to be highly labile. Compounds **2** and **3** are paramagnetic. Evans magnetic susceptibility measurements yielded a magnetic moment of  $3.2 \mu_B$  for both compounds. The value is consistent with an  $S = 1$   $\text{Ni}^{\text{II}}$  ion in the PDI site, alongside a diamagnetic  $\text{M}^{\text{II}}_{\text{Cyclam}}$  center ( $\text{M} = \text{Ni}^{\text{II}}$  (**2**);  $\text{Zn}^{\text{II}}$  (**3**)). The resonances of the  $^1\text{H}$  NMR spectra (Figure S21) appear in a broad range from  $-7$  – 210 ppm. The largest shifts and significant broadening are observed for the PDI protons, while the protons closest to the diamagnetic M–cyclam unit are less affected.

The electronic spectrum of **1** exhibits a characteristic trio of intense transitions centered at 300 nm, along with a lower energy feature at 352 nm, which all can be assigned as  $\pi$ - $\pi^*$  transitions associated with the Zn–PDI unit.<sup>11</sup> The Ni-containing **2** and **3** likewise exhibit PDI-based  $\pi$ - $\pi^*$  bands in this region.<sup>12</sup> The spectrum of **2** features additional absorptions at longer wavelengths ( $\lambda_{\text{max}} = 369, 461$  nm), as observed among Ni–cyclam complexes.<sup>13</sup> The spectrum of **3**, in contrast, lacks these distinctive visible absorption bands, whereas the higher energy spectral region ( $< 350$  nm) is nearly superimposable with that of **2**, providing further evidence that the  $\text{Ni}^{\text{II}}$  ion of the heterobimetallic complex resides in the PDI site. The Ni-containing compounds additionally exhibit broad bands in the NIR region, with  $\lambda_{\text{max}} = 948$  (**2**) and 960 (**3**) nm (Figure S23).

The incorporation of the redox-active PDI unit in the bimetallic framework offers access to a series of ligand-centered redox processes. In principal, the ligand can accept up to four electrons via its diimine  $\pi^*$  orbitals, associated with the electron transfer series,  $[\text{PDI}]^0 \rightarrow [\text{PDI}]^{4-}$ . Metal complexes coordinated by the mono- through tri-anionic forms have been identified.<sup>14</sup> The PDI unit acts as the sole electron storage site in the dizinc-containing **1**. Thus, the first one-electron reduction at  $-1.3$  V in the CV of **1** (CVs shown in Figure 2) corresponds to the formation of the monoanionic  $\text{PDI}^{\cdot-}$ , while the ensuing quasi-reversible couple at  $-1.7$  V can be assigned to the  $\text{PDI}^{\cdot-}/\text{PDI}^{2-}$  couple. Compound **2**, on the other hand, contains two  $\text{Ni}^{\text{II}}$  ions that can compete with the ligand for electrons. The CV of **2** depicts multiple redox events including a reversible metal-centered oxidation at  $+0.8$  V, as well as three reversible reductions at  $-0.9$ ,  $-1.4$ , and  $-1.6$  V.

The CV of **3** further helps to elucidate the nature of the redox processes. An oxidative event is absent in both the CVs of **1** and **3**, such that the one-electron oxidation of **2** ensues at the cyclam bound nickel center ( $\text{Ni}_{\text{Cy}}^{\text{III/II}}$ ). The absence of the oxidative couple in the CV of **3** is further evidence that the heterobimetallic complex is stable in solution – scrambling of the metal centers does not occur. The redox couples at  $-0.9$  V in the CV of both **2** and **3** seemingly can be attributed to the  $\text{Ni}_{\text{PDI}}^{\text{III/II}}$  couple, followed in each case by one-electron reduction of the PDI ligand ( $\text{PDI}/\text{PDI}^{\cdot-}$ ) at  $-1.4$  V. However, both ligand- and metal-centered one-electron reduced Ni-PDI complexes are described in the literature.<sup>12, 15</sup> The addition of the third electron to **2** occurs at  $-1.6$  V, and can be attributed to either the  $\text{PDI}^{\cdot-}/\text{PDI}^{2-}$  or  $\text{Ni}_{\text{Cy}}^{\text{II/I}}$  couples. The potential for one-electron reduction of related mono-nuclear cyclam compounds is highly dependent on the nature of additional ligands, but similar values were reported.<sup>16</sup> Since a third reductive event is not observed in the CV of **3**, reduction of the cyclam bound  $\text{Ni}^{\text{II}}$  ion likely accounts for the final redox process in the CV of **2**.

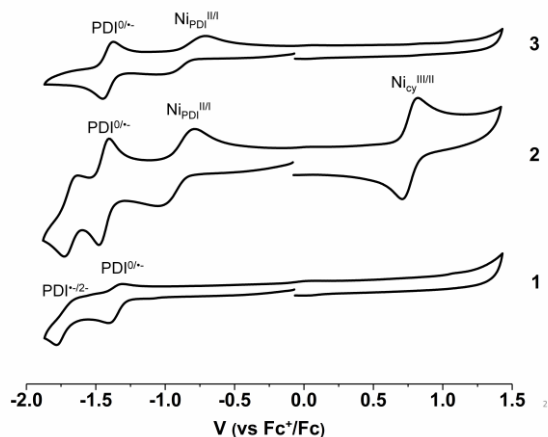


**Figure 2.** Cyclic voltammograms of **1** – **3** (MeCN, 0.5 mM complex 0.1 V s<sup>-1</sup>, 0.1 M  $[\text{N}(\text{n-Bu})_4]\text{PF}_6$ ).

We have thus far successfully isolated the one-electron forms of all three bimetallic compounds. The reduction of **1** was carried out using decamethylcobaltocene and yielded the bright orange complex  $[\text{Zn}_2(\text{PDIpCy})(\text{OTf})_3]$  (**4**). Compounds **2** and **3**, which possess more positive one-electron reduction potentials, were reduced using cobaltocene to produce the dark blue  $[\text{Ni}_2(\text{PDIpCy})(\text{OTf})](\text{OTf})_2$  (**5**) and  $[\text{NiZn}(\text{PDIpCy})(\text{OTf})_3]$  (**6**) (Scheme S3). CHN analytical and mass spectrometry data (see SI) verify the composition of the reduced compounds.

The solution electronic spectra of **4** – **6** (Figure S24) differ markedly from those of **1** – **3**. In contrast to the divalent **1**, the reduced **4** exhibits visible bands at  $\lambda_{\text{max}} = 492$  and 566 nm. The spectra of **5** and **6** display multi-structured features that encompass the full visible region, as well as NIR transitions up to ca. 1200 nm. The spectra of **4** – **6** further indicate that reduction of the divalent PDIpCy complexes occurs at the M(PDI) site in all three complexes.<sup>12, 15, 17</sup> However, with the exception of **4**, the question of ligand- vs. metal-centered reduction cannot be settled on the basis of the absorption spectra alone.

EPR spectroscopy resolves the electronic structures of **4** – **6**. A near anisotropic spectrum for **4** with  $g = (2.0105, 2.0060, 2.0005)$  is synonymous with a ligand-centered radical confined to the PDI portion of the ligand that is attached to a  $\text{Zn}^{\text{II}}$  ion (Figure S27). The room temperature spectra of **5** and **6** exhibit isotropic signals with  $g$ -values of 2.1512 and 2.1510, respectively, consistent with a  $d^9$  paramagnetic center (Figure 3, left). This electronic structure is confirmed by the frozen solution spectra recorded in an MeCN/toluene glass at 140 K (Figure 3, right). These spectra are

identical, and essentially axial with  $g = (2.2363, 2.1310, 2.0858)$  for **5**, and  $g = (2.2336, 2.1412, 2.0901)$  for **6**. The  $g_{\parallel} > g_{\perp} > g_e$  pattern is the hallmark of a  $\text{Ni}^{\text{I}}$  species with an unpaired electron in the  $\sigma^*$  MO of the Ni-PDI unit ( $d_{z^2}$  in  $C_{2v}$  symmetry). Therefore, **5** and **6** are mixed valent  $[\text{Ni}^{\text{I}}\text{Ni}^{\text{II}}(\text{PDIpCy})]^{3+}$  and  $[\text{Ni}^{\text{I}}\text{Zn}^{\text{II}}(\text{PDIpCy})]^{3+}$ , with a four-coordinate  $\text{Ni}^{\text{I}}$  ion at the PDI site, with the inclusion of a solvent molecule (MeCN) in the coordination sphere.<sup>15, 18</sup>

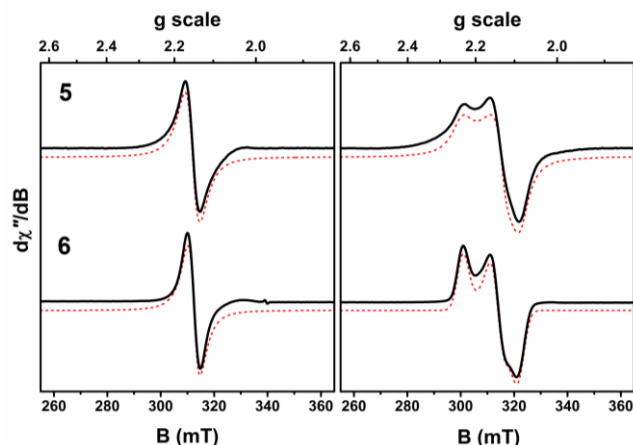


**Figure 3.** X-band EPR spectra of **5** and **6**. Left panel: MeCN solution at 293 K; right panel: MeCN/toluene frozen glass at 140 K. Experimental data are shown by the solid line; simulation depicted by the dashed trace (experimental conditions: frequency, 9.410 GHz; modulation, 0.5 mT; power, 0.63 mW).

The results of studies with the series of M-PDIpCy compounds already highlight several unique features of our new ligand system. The metal ions in **1** – **3** are physically connected via the propyl linker, but electronically uncoupled. The compounds afford disparate coordination environments, including variations in the number and orientation of labile coordination sites. It should indeed be feasible to individually tune the properties of each site for discrete functions. Nevertheless, we speculate that the flexible propyl bridge separating the two coordination sites might permit cooperative interactions under appropriate conditions, e.g. in the presence of suitable substrates or added ligands that could bind in a bridging fashion. Compounds **5** and **6** represent conventional metal-centered, mixed valence ( $\text{Ni}_{\text{PDI}}^{\text{I}}\text{Ni}_{\text{Cy}}^{\text{II}}$ ,  $\text{Ni}_{\text{PDI}}^{\text{I}}\text{Zn}_{\text{Cy}}^{\text{II}}$ ) complexes. In contrast, charge localization also ensues in **4**, but via electron storage at the PDI ligand ( $[\text{Zn}^{\text{II}}((\text{PDI}^{\cdot-})\text{pCy})\text{Zn}^{\text{II}}]^+$ ). All three complexes are thus primed for redox reactions at the  $\text{M}_{\text{PDI}}$  site; the  $\text{M}_{\text{Cy}}$  center could potentially act in a Lewis acid capacity. The electrochemistry data imply that two-electron charge localized species also are accessible, since at least the first two electrons are consistently taken up by the M-PDI unit of **1** – **3**. The generation of such *formally* two-electron mixed-valent  $\text{M}^{\text{0}}_{\text{PDI}}\cdots\text{M}^{\text{II}}_{\text{Cy}}$  species could offer significant advantages for multi-electron reactions.<sup>19</sup> Aspects concerning reactivity, as well as the formation of additional heterobimetallic compounds, will subsequently be explored.

## ASSOCIATED CONTENT

### Supporting Information

The supporting material is available free of charge via the Internet at <http://pubs.acs.org>.

Detailed experimental procedures, analytical data, spectra and X-ray crystallographic data.

### Accession Codes

CCDC 1572803 – 1572805 contain the supplementary crystallographic data for this paper. These data can be obtained free of charge via [www.ccdc.cam.ac.uk/data\\_request/cif](http://www.ccdc.cam.ac.uk/data_request/cif), or by emailing [data\\_request@ccdc.cam.ac.uk](mailto:data_request@ccdc.cam.ac.uk), or by contacting The Cambridge Crystallographic Data Centre, 12 Union Road, Cambridge CB21EZ, UK; fax: +44 1223 336033.

## AUTHOR INFORMATION

### Corresponding Author

\* Email: [corinna.hess@ch.tum.de](mailto:corinna.hess@ch.tum.de)

### Present address

ZH: Department of Chemistry and Biochemistry, University of California, Los Angeles, CA 90095, USA.

### Notes

The authors declare no competing financial interests.

## ACKNOWLEDGMENT

RMH thanks the TUM Graduate School for financial support. ZH gratefully acknowledges the NSF NanoRing program (IRES-1460031), coordinated by the TUM IGSSE, for funding. Our thanks go to Dr A. Pöthig and his team for help with X-ray crystallography and to Dr. C. Hæßner for technical assistance with EPR measurements.

## REFERENCES

(1) (a) Barber, J. The Mn<sub>2</sub>Ca-cluster of the photosynthetic oxygen evolving centre: its structure, function and evolution. *Biochem.* **2016**, *55*, 5901-5906. (b) Lubitz, W.; Ogata, H.; Rüdiger, O.; Reijerse, E. Hydrogenases. *Chem. Rev.* **2014**, *114*, 4081-4148. (c) Hoffman, B. M.; Lukoyanov, D.; Yang, Z. Y.; Dean, D. R.; Seefeldt, L. C. Mechanism of nitrogen fixation by nitrogenase: the next stage. *Chem. Rev.* **2014**, *114*, 4041-4062. (d) Hess, C. R.; Welford, R. W. D.; Klinman, J. P.; Begley, T. P. In *Wiley Encyclopedia of Chemical Biology*; John Wiley & Sons, Inc.: 2007; 529-540.

(2) (a) Blakemore, J. D.; Crabtree, R. H.; Brudvig, G. W. Molecular catalysts for water oxidation. *Chem. Rev.* **2015**, *115*, 12974-13005. (b) Barrière, F. In *Bioinspired Catalysis: Metal-Sulfur Complexes*; W. Weigand, P. S., Ed.; Wiley-VCH Verlag GmbH & Co. KGaA: 2015; Chapter 9, 225-248. (c) Friedle, S.; Reisner, E.; Lippard, S. J. Current challenges of modeling diiron enzyme active sites for dioxygen activation by biomimetic synthetic complexes. *Chem. Soc. Rev.* **2010**, *39*, 2768-2779. (d) Das, B.; Daver, H.; Singh, A.; Singh, R.; Haukka, M.; Demeshko, S.; Meyer, F.; Lisensky, G.; Jarenmark, M.; Himo, F.; Nordlander, E. A Heterobimetallic Fe<sup>III</sup>Mn<sup>II</sup> Complex of an Unsymmetrical Dinucleating Ligand: A Structural and Functional Model Complex for the Active Site of Purple Acid Phosphatase of Sweet Potato. *Eur. J. Inorg. Chem.* **2014**, *2014*, 2204-2212. (e) Quist, D. A.; Diaz, D. E.; Liu, J. J.; Karlin, K. D. Activation of dioxygen by copper metalloproteins and insights from model complexes. *J. Biol. Inorg. Chem.* **2017**, *22*, 253-288.

(3) (a) Krogman, J. P.; Thomas, C. M. Metal-metal multiple bonding in C<sub>3</sub>-symmetric bimetallic complexes of the first row transition metals. *Chem. Commun.* **2014**, *50*, 5115-5127. (b) Rosenkoetter, K. E.; Ziller, J. W.; Heyduk, A. F. A Heterobimetallic W-Ni Complex Containing a Redox-Active W[SNS]<sub>2</sub> Metalloligand. *Inorg. Chem.* **2016**, *55*, 6794-6798. (c) Dunn, P. L.; Carlson, R. K.; Gagliardi, L.; Tonks, I. A. Structure and bonding of group 4-nickel heterobimetallics supported by 2-(diphenylphosphino)pyrrolide ligands. *Dalton Trans.* **2016**, *45*, 9892-9901. (d) Berry, J. F.; Lu, C. C. Metal-Metal Bonds: From Fundamentals to Applications. *Inorg. Chem.* **2017**, *56*, 7577-7581.

(4) For examples see: (a) Zhang, H.; Dechert, S.; Maurer, J.; Linseis, M.; Winter, R. F.; Meyer, F. Heterobimetallic Mn/Co hybrid complexes composed of proximate organometallic and classical coordination sites. *J. Organomet. Chem.* **2007**, *692*, 2956-2964. (b) Wang, D.; Lindeman, S. V.; Fiedler, A. T. Synthesis of homo- and heterobimetallic Ni<sup>II</sup>-M<sup>II</sup> (M = Fe, Co, Ni, Zn) complexes based on an asymmetric ligand framework: Structures, spectroscopic features, and redox properties. *Inorg. Chim. Acta*

**2014**, *421*, 559-567. (c) Roth, A.; Buchholz, A.; Rudolph, M.; Schütze, E.; Kothe, E.; Plass, W. Directed Synthesis of a Heterobimetallic Complex Based on a Novel Unsymmetric Double-Schiff-Base Ligand: Preparation, Characterization, Reactivity and Structures of Hetero- and Homobimetallic Nickel(II) and Zinc(II) Complexes. *Chem. Eur. J.* **2008**, *14*, 1571-1583. (d) Roth, A.; Spielberg, E. T.; Plass, W. Kit for Unsymmetric Dinucleating Double-Schiff-Base Ligands: Facile Access to a Versatile New Ligand System and Its First Heterobimetallic Copper-Zinc Complex. *Inorg. Chem.* **2007**, *46*, 4362-4364.

(5) (a) Lin, P.-H.; Takase, M. K.; Agapie, T. Investigations of the Effect of the Non-Manganese Metal in Heterometallic-Oxido Cluster Models of the Oxygen Evolving Complex of Photosystem II: Lanthanides as Substitutes for Calcium. *Inorg. Chem.* **2015**, *54*, 59-64. (b) Cook, S. A.; Borovik, A. S. Molecular designs for controlling the local environments around metal ions. *Acc. Chem. Res.* **2015**, *48*, 2407-2414. (c) Delgado, M.; Ziegler, J. M.; Seda, T.; Zakharov, L. N.; Gilbertson, J. D. Pyridinediimine Iron Complexes with Pendant Redox-Inactive Metals Located in the Secondary Coordination Sphere. *Inorg. Chem.* **2016**, *55*, 555-557. (d) Connor, G. P.; Holland, P. L. Coordination chemistry insights into the role of alkali metal promoters in dinitrogen reduction. *Catal. Today* **2017**, *286*, 21-40.

(6) (a) Cammarota, R. C.; Clouston, L. J.; Lu, C. C. Leveraging molecular metal-support interactions for H<sub>2</sub> and N<sub>2</sub> activation. *Coord. Chem. Rev.* **2017**, *334*, 100-111. (b) Krogman, J. P.; Bezpalko, M. W.; Foxman, B. M.; Thomas, C. M. Multi-electron redox processes at a Zr(IV) center facilitated by an appended redox-active cobalt-containing metalloligand. *Dalton Trans.* **2016**, *45*, 11182-11190.

(7) (a) Barefield, E. K. Coordination chemistry of N-tetraalkylated cyclam ligands—A status report. *Coord. Chem. Rev.* **2010**, *254*, 1607-1627. (b) Cho, J.; Sarangi, R.; Nam, W. Mononuclear Metal O<sub>2</sub> Complexes Bearing Macrocyclic N-Tetramethylated Cyclam Ligands. *Acc. Chem. Res.* **2012**, *45*, 1321-1330. (c) Chirik, P. J. In *Pincer and Pincer-Type Complexes: Applications in Organic Synthesis and Catalysis*; Szabo, K. J., Wendt, O. F., Ed.; Wiley-VCH Verlag GmbH & Co. KGaA: 2014; Chapter 7, 189-212.

(8) (a) Chen, L.; Chen, G.; Leung, C.-F.; Yiu, S.-M.; Ko, C.-C.; Anxolabéhère-Mallart, E.; Robert, M.; Lau, T.-C. Dual Homogeneous and Heterogeneous Pathways in Photo- and Electrocatalytic Hydrogen Evolution with Nickel(II) Catalysts Bearing Tetradentate Macrocyclic Ligands. *ACS Catal.* **2015**, *5*, 356-364. (b) Schneider, J.; Jia, H.; Kobiros, K.; Cabelli, D. E.; Muckerman, J. T.; Fujita, E. Nickel(II) macrocycles: highly efficient electrocatalysts for the selective reduction of CO<sub>2</sub> to CO. *Energ. & Environ. Sci.* **2012**, *5*, 9502-9510. (c) Lee, D.; Bang, H.; Suh, M. P. Epoxidation of an alkene promoted by various nickel(II) multi-azamacrocyclic complexes. *J. Mol. Catal. A* **2000**, *151*, 71-78. (d) McCrory, C. C. L.; Szymczak, N. K.; Peters, J. C. Evaluating Activity for Hydrogen-Evolving Cobalt and Nickel Complexes at Elevated Pressures of Hydrogen and Carbon Monoxide. *Electrocatal.* **2015**, *7*, 87-96.

(9) Bianchini, C.; Mantovani, G.; Meli, A.; Migliacci, F.; Zanobini, F.; Laschi, F.; Somazzi, A. Oligomerisation of Ethylene to Linear  $\alpha$ -Olefins by new Cs- and Cl-Symmetric [2,6-Bis(imino)pyridyl]iron and -cobalt Dichloride Complexes. *Eur. J. Inorg. Chem.* **2003**, *2003*, 1620-1631.

(10) (a) Baidya, N.; Olmstead, M. M.; Mascharak, P. K. A Mononuclear Nickel(II) Complex with [NiN<sub>3</sub>S<sub>2</sub>] Chromophore That Readily Affords the Ni(I) and Ni(III) Analogues: Probe into the Redox Behavior of the Nickel Site in [FeNi] Hydrogenases. *J. Am. Chem. Soc.* **1992**, *114*, 9666-9668. (b) Coggin, D. K.; Gonzalez, J. A.; Kook, A. M.; Stanbury, D. M.; Wilson, L. J. Ligand Dynamics in Pentacoordinate Copper(I) and Zinc(II) Complexes. *Inorg. Chem.* **1991**, *30*, 1115-1125. (c) Davis, R. N.; Tanski, J. M.; Adrian, J. C.; Tyler, L. A. Variations in the coordination environment of Co<sup>2+</sup>, Cu<sup>2+</sup> and Zn<sup>2+</sup> complexes prepared from a tridentate (imino)pyridine ligand and their structural comparisons. *Inorg. Chim. Acta* **2007**, *360*, 3061-3068. (d) Crick, I. S.; Gable, R. W.; Hoskins, B. F.; Tregloan, P. A. The Crystal Structure of 1,4,8,11-Tetramethyl-1,4,8,11-tetraazacyclotetradecane Nickel(II) Bis(perchlorate) at 155 K. *Inorg. Chim. Acta* **1986**, *111*, 35-38. (e) Hambley, T. W. The Crystal Structure of R,S,R,S-(1,4,8,11-Tetramethyl-1,4,8,11-tetraazacyclotetradecane) nickel (II) Bis(trifluoromethanesulphonate)-Acetone Hydrate, [Ni(tmtactd)] [CF<sub>3</sub>SO<sub>3</sub>]<sub>2</sub>·Me<sub>2</sub>CO·H<sub>2</sub>O, and a Strain-energy Minimization Analysis of Four-, Five-, and Six-coordinate Nickel(II)-tmtactd Solvento Complexes *J. Chem. Soc. Dalton Trans.* **1986**, 565-569. (f) Kim, J. C.; Lough, A. J.; Park, H.; Kang, Y. C. Molecular interactions of zinc(II) cyclams toward maleate and fumarate anions. *Inorg. Chem. Commun.* **2006**, *9*, 514-517. (g) Kannappan, R.; Rousselin, Y.; Jabri, R. Z.; Goze, C.; Brandès, S.; Guillard, R.; Zrineh, A.; Denat, F.

Synthesis, structure and coordination properties of three cyclam-based ligands bearing one scorpionate arm. *Inorg. Chim. Acta* **2011**, *373*, 150-158.

(11) Delgado, M.; Sommer, S. K.; Swanson, S. P.; Berger, R. F.; Seda, T.; Zakharov, L. N.; Gilbertson, J. D. Probing the Protonation State and the Redox-Active Sites of Pendant Base Iron(II) and Zinc(II) Pyridinediimine Complexes. *Inorg. Chem.* **2015**, *54*, 7239-7248.

(12) Ghosh, M.; Weyhermüller, T.; Wieghardt, K. Electronic structure of the members of the electron transfer series  $[\text{NiL}]^z$  ( $z = 3+, 2+, 1+, 0$ ) and  $[\text{NiL}(\text{X})]^n$  ( $\text{X} = \text{Cl}, \text{CO}, \text{P}(\text{OCH}_3)_3$ ) species containing a tetradentate, redox-noninnocent, Schiff base macrocyclic ligand L: an experimental and density functional theoretical study. *Dalton Trans.* **2010**, *39*, 1996-2007.

(13) (a) Boiocchi, M.; Fabbri, L.; Foti, F.; Vazquez, M. Further insights on the high-low spin interconversion in nickel(II) tetramine complexes. Solvent and temperature effects. *Dalton Trans.* **2004**, 2616-2620. (b) Ciampolini, M.; Fabbri, L.; Licchelli, M.; Perotti, A.; Pezzini, F.; Poggi, A. Steric Effects on the Solution Chemistry of Nickel(II) Complexes with N-Monomethylated 14-Membered Tetraaza Macrocycles. The Blue-to-Yellow Conversion and the Oxidation and Reduction Behavior. *Inorg. Chem.* **1986**, *25*, 4131-4135.

(14) (a) Enright, D.; Gambarotta, S.; Yap, G. P. A.; Budzelaar, P. H. M. The Ability of the  $\alpha,\alpha'$ -Diiminopyridine Ligand System to Accept Negative Charge: Isolation of Paramagnetic and Diamagnetic Trianions. *Angew. Chem. Int. Ed.* **2002**, *41*, 3873-3876. (b) Knijnenburg, Q.; Gambarotta, S.; Budzelaar, P. H. Ligand-centred reactivity in diiminepyridine complexes. *Dalton Trans.* **2006**, 5442-5448. (c) Chirik, P. J.; Wieghardt, K. Radical Ligands Confer Nobility on Base-Metal Catalysts. *Science* **2010**, *327*, 794-795.

(15) Lewis, J.; Schröder, M. Reduction of Schiff-base macrocyclic complexes. Stabilisation of nickel(I) conjugated macrocyclic complexes via a reversible ligand-to-metal electron-transfer process. *Dalton Trans.* **1982**, 1085-1089.

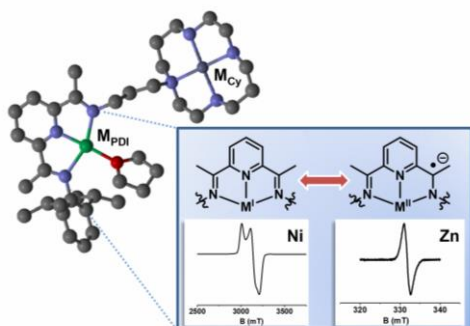
(16) (a) Blake, A. J.; Gould, R. O.; Hyde, T. I.; Schröder, M. Stabilisation of Monovalent Palladium by Tetra-aza Macrocycles. *J. Chem. Soc., Chem. Commun.* **1987**, 431-433. (b) El Ghachtouli, S.; Cadiou, C.; Déchamps-Olivier, I.; Chuburu, F.; Aplincourt, M.; Turcry, V.; Le Baccon, M.; Handel, H. Spectroscopy and Redox Behaviour of Dicopper(II) and Dinickel(II) Complexes of Bis(cyclen) and Bis(cyclam) Ligands. *Eur. J. Inorg. Chem.* **2005**, *2005*, 2658-2668. (c) Barefield, E. K.; Freeman, G. M.; Van Derveer, D. G. Electrochemical and Structural Studies of Nickel(II) Complexes of N-Alkylated Cyclam Ligands: X-ray Structures of trans  $[\text{Ni}(\text{C}_{14}\text{H}_{32}\text{N}_4(\text{OH}_2)_2)\text{Cl}_2 \cdot 2\text{H}_2\text{O}]$  and  $[\text{Ni}(\text{C}_{14}\text{H}_{32}\text{N}_4)(\text{O}_3\text{SCF}_3)_2]$ . *Inorg. Chem.* **1986**, *25*, 552-558.

(17) Manuel, T. D.; Rohde, J.-U. Reaction of a Redox-Active Ligand Complex of Nickel with Dioxygen Probes Ligand-Radical Character. *J. Am. Chem. Soc.* **2009**, *131*, 15582-15583.

(18) (a) Marganian, C. A.; Vazir, H.; Baidya, N.; Olmstead, M. M.; Mascharak, P. K. Toward Functional Models of the Nickel Sites in [FeNi] and [FeNiSe] Hydrogenases: Syntheses, Structures, and Reactivities of Nickel(II) Complexes Containing  $[\text{NiN}_3\text{S}_2]$  and  $[\text{NiN}_3\text{Se}_2]$  Chromophores. *J. Am. Chem. Soc.* **1995**, *117*, 1584-1594. (b) Ciszewski, J. T.; Mikhaylov, D. Y.; Holin, K. V.; Kadirov, M. K.; Budnikova, Y. H.; Sinyashin, O.; Vicic, D. A. Redox Trends in Terpyridine Nickel Complexes. *Inorg. Chem.* **2011**, *50*, 8630-8635.

(19) (a) Dempsey, J. L.; Esswein, A. J.; Manke, D. R.; Rosenthal, J.; Soper, J. D.; Nocera, D. G. Molecular Chemistry of Consequence to Renewable Energy. *Inorg. Chem.* **2005**, *44*, 6879-6892. (b) Rosenthal, J.; Bachman, J.; Dempsey, J. L.; Esswein, A. J.; Gray, T. G.; Hodgkiss, J. M.; Manke, D. R.; Lockett, T. D.; Pistorio, B. J.; Veige, A. S.; Nocera, D. G. Oxygen and hydrogen photocatalysis by two-electron mixed-valence coordination compounds. *Coord. Chem. Rev.* **2005**, *249*, 1316-1326.

## For Table of Contents Only



The new ligand, PDIpCy, offers two distinct, non-coupled coordination sites: a redox-active pyridyldiimine (PDI) group and a cyclam (Cy) unit. The series of homo- and heterobimetallic Ni- and Zn-PDIpCy complexes described herein, includes charge-separated forms.